# Structural Evolution of a Model Poly(imide): Organization near Surfaces

**David C. Martin,* Larry L. Berger, and Kenncorwin H. Gardner**

*Central Research and Development, E. I. du Pont de Nemours and Company, Wilmington, Delaware 19880-0356*

*Received October 25, 1990; Revised Manuscript Received February 11, 1991*

ABSTRACT: Details of the molecular organization occurring during imidization of the poly(amic acid) PMDA-12C at temperatures below the bulk melting point were examined. In particular, the effects of surface constraints were investigated by studying structural evolution in thin droplets. Scanning electron microscopy (SEM) and transmission electron microscopy (TEM) experiments on as-cast and imidized droplets illustrated the development of surface roughness and fluctuations in mass thickness. High-resolution electron microscopy (HREM) studies near the droplet edge showed discrete crystallites containing uniformly spaced 1.8-nm (001) fringes, which correspond to the repeat distance along the polymer backbone. The projected size, shape, orientation, and relative population of the crystallites were analyzed quantitatively. The crystallites were found to be slightly extended in the axial direction, with an average axial dimension of 53 ± 23 nm and average lateral dimension of 38 ± 13 nm. The polymer chains within 100 nm of the droplet edge were found to be strongly oriented in the plane of the droplet and weakly oriented parallel to the droplet edge. Certain crystallites appeared to contain internal bending deformation (with the radius of curvature as small as 50 nm). Evidence for different types of grain boundaries between adjacent crystallites was obtained. On the basis of these observations, the molecular structure of crystallite interfaces and their possible influence on the physical properties of crystallizable polymers are discussed.

## Introduction

The near-surface structure of polymers is important for determining properties such as adhesion, transport, friction, and fracture initiation. The influence of a surface on the conformations of polymer molecules has been the subject of both theoretical and experimental interest. For example, Theodorou has investigated the polymer melt/free surface interface using a variable-density lattice model and predicts perturbations in the density and orientation of the chains in the region immediately adjacent to the surface.[1] Henkee et al. have found that block copolymers can exhibit novel microphase separation behavior when confined into thin droplets.[2] In glassy polymers Berger and Sauer have shown that segmental relaxations of chains on or near a free surface can be greatly enhanced relative to those of the bulk polymer.[3]

Information about surface structure should prove particularly important for understanding the properties of poly(imides), which are often used as temperature-resistant dielectric barriers, adhesives, and hollow fiber membranes. Typically, poly(imides) are prepared by casting films of the poly(amic acid) precursor and subsequently converting to poly(imide) either thermally or chemically. The general reaction scheme is shown in Figure 1. Imidization involves the simultaneous loss of solvent and cyclization of the dianhydride moiety and can result in crystallization or orientation. However, because of the general intractability and limited crystallinity of commercially important poly(imides), e.g., PMDA-ODA, it has been difficult to develop a detailed understanding of the factors that control structure and properties.

We have investigated the evolution of the microstructure and properties during thermal imidization of PMDA-12C, which is a poly(imide) prepared from pyromellitic dianhydride (PMDA) and a twelve-carbon aliphatic diamine (12C). The chemical structures of these repeat units as well as the aromatic dianhydride oxydianyline (ODA)

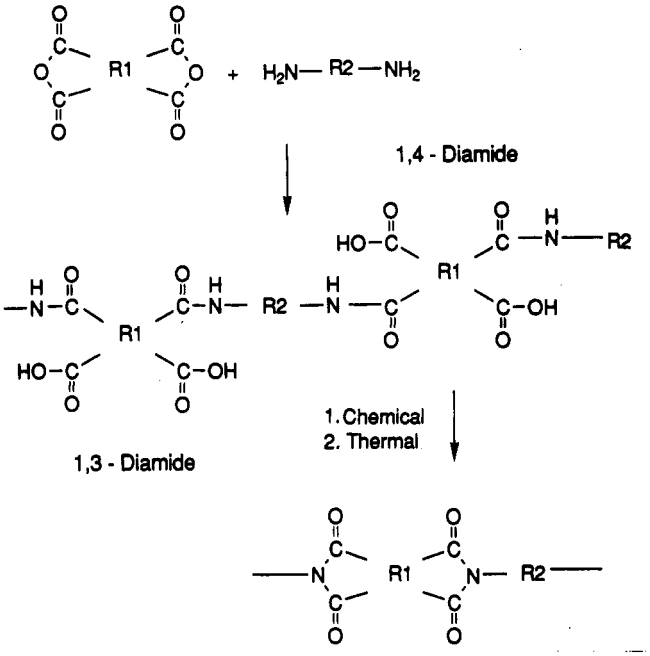


**Figure 1.** General reaction scheme for the preparation of poly(imides). A dianhydride and a diamine are combined to make a poly(amic acid) precursor that has 1,3-diamide and 1,4-diamide linkages. The poly(amic acid) polymer is cast into a film and then converted thermally or chemically into the poly(imide).

are shown in Figure 2. In contrast to PMDA-ODA, PMDA-12C has experimentally accessible transition temperatures, thus allowing the morphology obtained by crystallization during imidization to be compared with that obtained by crystallization from the melt.

In previous work, we examined the crystallization of thick films (~25 μm) of PMDA-12C by wide-angle X-ray scattering (WAXS) and optical microscopy (OM).[4] From these studies it was apparent that the morphology that developed during imidization below the bulk melting point was not the typical spherulitic texture normally found in polymers crystallized from the melt. However, it was not

* Address correspondence to this author at: Materials Science and Engineering, The University of Michigan, H. H. Dow Building, Ann Arbor, MI 48109-2136.

0024-9297/91/2224-3921$02.50/0 

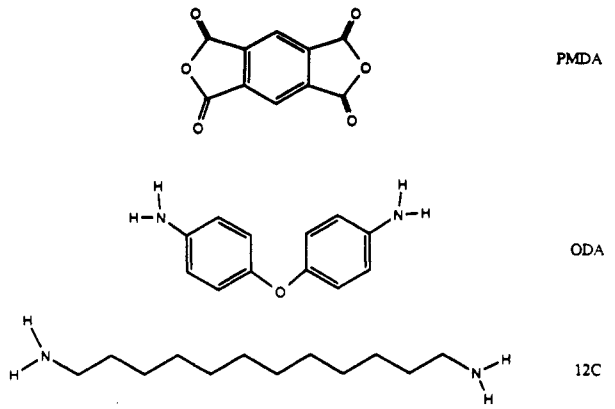


**Figure 2.** Chemical structure of the dianhydride PMDA and the diamines ODA and 12C.

possible to obtain details about the local size, shape, and relative orientation of the crystallites that were formed nor could the possible effect of surface constraints on the microstructure be deduced.

Here, we report on our direct observations of the molecular organization that occurs during imidization of PMDA-12C using electron microscopy. In particular, we explore the effect of surfaces by examining the microstructure near the edges of thin droplets. With this geometry it is possible to isolate the effect of the surface and minimize problems associated with conventional sample preparation techniques and image interpretation.

## Experimental Section

The poly(amic acid) precursor polymer was prepared by condensation polymerization; the details of this synthesis are given elsewhere.[4] The PMDA-12C poly(amic acid) used in this study had an IV of 0.57 dL/g, with an estimated $M_n$ of ~3560 and $M_w$ ~25 600. The molecular weights were determined by gel permeation chromatography (GPC) using the procedure of Walker.[5]

Thick films (~25 μm) of the PMDA-12C poly(amic acid) were prepared by spinning a 20 wt % solution in 1-methyl-2-pyrrolidinone (NMP) onto glass (clean microscope slides) or single-crystal quartz substrates. The films were allowed to dry at room temperature. The as-cast films were converted to poly(imide) by thermal annealing for various temperatures and times in a vacuum oven. WAXS diffractometer scans were collected in the symmetrical reflection mode by using an automated Philips diffractometer (curved crystal monochromator, 1/4° divergence and receiving slits, sample rotating) and Cu Kα radiation. Data were collected in a fixed-time mode with a step size of 0.02° 2θ from scattering angles of 2.5–50° 2θ.

A stock solution of 20 wt % of PMDA-12C poly(amic acid) in 1-methyl-2-pyrrolidinone (NMP) was diluted to 0.1 wt % with additional NMP. Droplets of polymer were prepared by atomizing this dilute solution onto mica substrates that had been previously cleaved and then coated with approximately 20 nm of amorphous carbon in a Denton bench top turbo vacuum evaporator ($10^{-5}$ Torr). After drying at room temperature, selected samples were annealed at various temperatures under vacuum. The carbon support film was floated off the mica substrate onto distilled water and then lifted onto 400-mesh copper grids.

The surface structure of the droplets was examined with a Hitachi S-800 scanning electron microscope (SEM) operating at 2 kV. This low operating voltage minimized charging effects so that the samples could be imaged directly, thus eliminating the need for a conductive metallic coating that might obscure high-resolution surface detail. The images were obtained with a secondary electron detector.

Higher resolution information about the droplet structure was obtained with a JEOL 2000 EX transmission electron microscope (TEM) operating at 200 kV. Samples were examined both uncoated and shadowed at a low incident angle (10–12°) with silver.

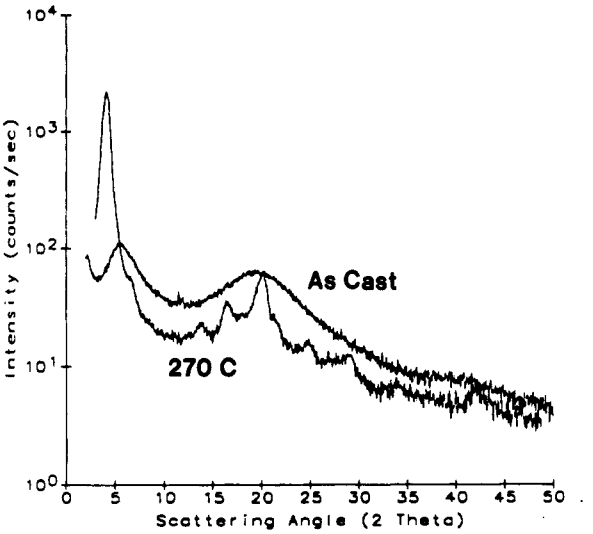


**Figure 3.** WAXS diffractometer scans of PMDA-12C cast as poly(amic acid) film and after imidization for 1 h at 270 °C.

The silver was deposited by heating 10 mm of 0.2-mm diameter silver wire that was held above the sample with a tungsten basket in the vacuum evaporator.

By measuring the time necessary for fading of the (001) reflection in selected area electron diffraction (SAED) at a known incident beam flux, it was found that the total end point dose (TEPD) of PMDA-12C was 0.02 C/cm² for 200-kV electrons at room temperature. Since the melting point of PMDA-12C is 312 °C, this is in general agreement with the empirical correlation of the electron beam damage resistance of polymers with thermal stability presented by Kumar and Adams.[6]

Low dose, high-resolution electron microscopy (HREM) was used to image the (001) spacings, which were independently determined (by flat film WAXS of oriented samples) to correspond to the monomer repeat distance along the chain axis.[4] Micrographs were obtained with the plane of the droplet perpendicular to the electron beam. A relatively low magnification of 25000× minimized the exposure of the sample to the electron beam. For an optical density of 0.8 on Kodak SO-163 electron image film, a beam flux at the sample of 0.004 C/cm² was required.

The specific experimental procedures for successful low-dose HREM of polymers have been described elsewhere in detail.[7] Briefly, suitable areas for imaging were found by searching the sample with a defocused diffraction spot at low beam flux. Final focusing was adjusted on an area of the carbon film adjacent to the sample. The beam was then deflected at the condensor lens level by using a beam blanking device, and the microscope was allowed to come to mechanical equilibrium (approximately 5 min).

For imaging a sample with a known periodicity $d$, which is well above the theoretical resolution limit of the microscope, it is useful not to image at Scherzer focus[8] (for highest resolution) but rather to maximize the phase contrast by using an objective lens underfocus of $d^2/2\lambda$. For PMDA-12C the $d$ spacings of the (001) reflection measured using WAXS ranged from 1.6 to 2.1 nm,[4] giving the optimum amount of underfocus as 510–880 nm for 200-kV electrons ($\lambda = 2.51 \times 10^{-3}$ nm).

The presence of lattice fringes on the low-dose HREM negatives was confirmed by optical diffraction using a He–Ne laser optical bench. The spacings of the fringes in the HREM images of PMDA-12C were calibrated with a 6.85-nm lattice image of a catalase crystal standard[9] taken at the same magnification.

## Results

Figure 3 shows WAXS diffractometer scans of PMDA-12C poly(amic acid) films as cast and after thermal conversion to the poly(imide) by heating for 1 h at 270 °C.[4] The strong low-angle peak near 2θ = 5° in the poly(amic acid) pattern was observed to shift to lower angle, increase in height, and decrease in width during conversion

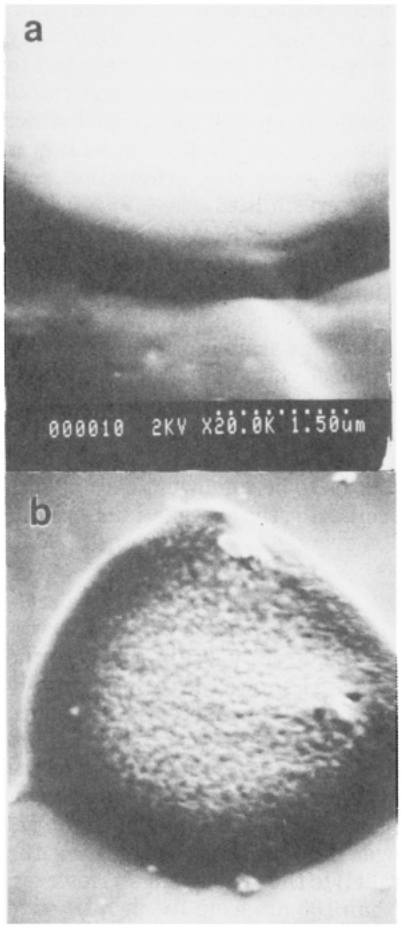


**Figure 4.** SEM micrograph of as-cast and heat-treated droplets. Heat treatment causes a roughening of the sample surface with undulations that are approximately 50 nm.

to poly(imide). Flat-film WAXS patterns from uniaxially oriented films showed that this reflection was oriented parallel to the gross orientation axis, indicating that the peak corresponded to the (001) repeat distance along the polymer backbone. This assignment indicated that there was one monomer repeat per unit cell in the direction of orientation, consistent with a crystal structure involving lateral association of rigid and flexible segments into discrete planes nominally perpendicular to the chain axis. From the Scherrer relationship, an effective crystallite size in the (001) direction of 2 nm was measured for as-cast samples and 7.5 nm for samples thermally treated at 270 °C.

SEM micrographs of droplets before and after heat treatment for 1 h at 210 °C are shown in Figure 4. Independent measurements of the reaction kinetics by Fourier transform infrared spectroscopy (FTIR) indicated that this heat treatment was sufficient to cause virtually complete imidization.[4] The surface of the original poly(amic acid) droplet was found to be smooth and relatively featureless, with a sharp interface between the droplet and the carbon support film. On the other hand, the heat-treated droplet showed rough surface undulations. The undulations did not seem periodic or organized in any particular manner. Close inspection of the micrograph revealed that the characteristic size of these undulations was on the order of 50 nm. From the HREM observations we will discuss later, this length scale roughly corresponds to the size of PMDA-12C crystallites.

A bright field TEM image of a droplet of the as-cast PMDA-12C shadowed with silver is shown in Figure 5. The uniform metal coverage indicated that the wetting

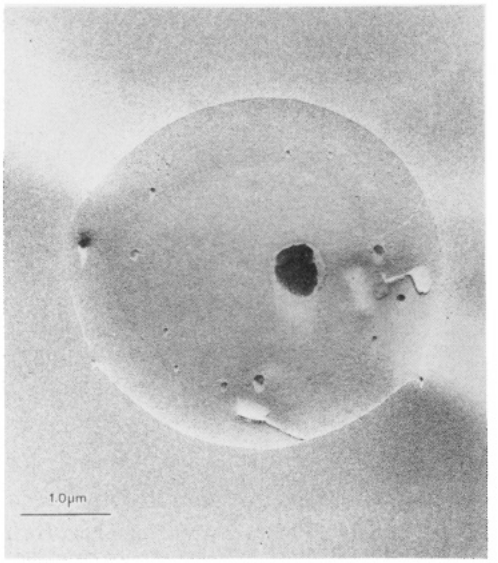


**Figure 5.** Bright field TEM micrograph of an as-cast poly(amic acid) droplet, shadowed with silver at an incident angle of 10°. The surface is smooth, indicating a low wetting angle and nearly flat droplet. There is a slight curvature near the very edge of the droplet as indicated by a lack of shadowing in this area.

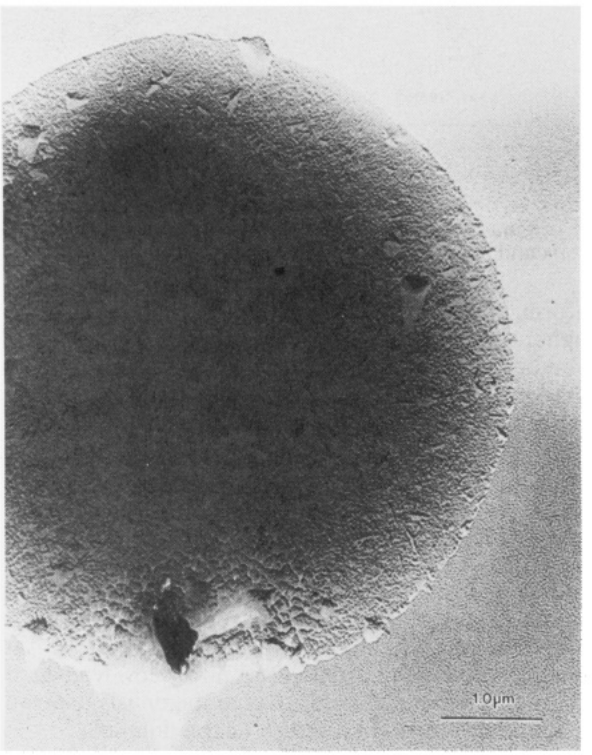


**Figure 6.** Bright field TEM micrograph of a heat-treated poly(imide) droplet, shadowed with silver at an incident angle of 10°. The roughness of the surface is immediately evident, as well as a buildup of metal on the leading edge and shadow on the trailing edge of the droplet. These observations are consistent with a small step at the droplet edge.

angle of the droplet with respect to the carbon substrate was small (less than 10°) and the droplet surface was smooth. Observations near the trailing edge of the droplet showed that there was a dearth of metal in the outermost 75 nm, indicating a slight downward curvatuve of the droplet surface in this region. The droplet surface and outermost edge were smooth down to a length scale of approximately 2 nm.

Figure 6 shows a shadowed droplet of PMDA-12C heat treated for 1 h at 210 °C. Again the metal coverage was

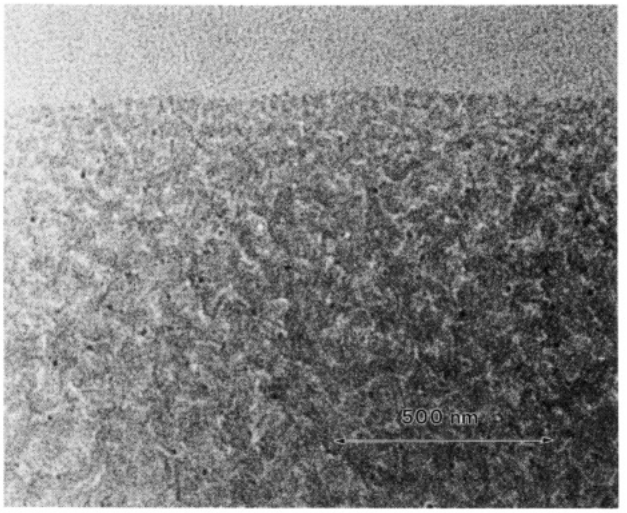


**Figure 7.** Bright field TEM micrograph of a heat-treated, uncoated droplet. Note the mottled appearance near the droplet edge, indicating a reorganization of the material into discrete domains with different projected mass thickness.

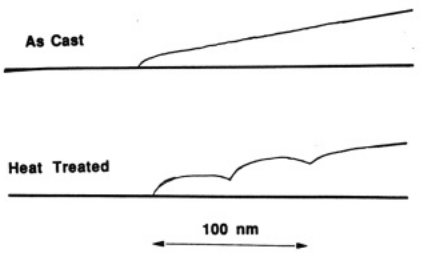


**Figure 8.** Schematic of droplet profile during heat treatment. The originally smooth as-cast droplet develops surface undulations and a step at the edge when heat treated.

uniform, but here the surface of the droplet was noticeably rougher than that of the as-cast droplet. There was also a buildup of metal on the front edge of the droplet and a shadow on the trailing edge, indicating a "step" in the sample height at the droplet edge. From the width of the shadow (20–60 nm) and the angle of shadowing (10°), the size of this step was determined to be 7 ± 4 nm.

In low-resolution bright field imaging of uncoated, heat-treated droplets it was possible to discern texture due to "domains" in the thinnest regions near the edge of the droplet, as shown in Figure 7. These domains corresponded to local areas within the droplet having a different mass thickness. Again, the approximate size of these domains was on the order of 50 nm. However, at this resolution it was not possible to unambiguously determine the shape or internal structure of the domains.

A schematic profile of the droplet based on these quantitative observations is shown in Figure 8. Originally, the as-cast droplet was flat and smooth with downward curvature of its surface in the outermost 75 nm. In contrast, the heat-treated droplet exhibited surface undulations in SEM and discrete areas of domains with higher mass thickness in TEM. Additionally, for the heat-treated droplet there was a step at the edge on the order of 7 nm, and the characteristic dimension of the surface undulations was on the order of 50 nm.

A low-dose HREM image of the droplet edge showing areas of well-defined (001) lattice fringes is presented in Figure 9a. These fringes were of uniform spacing (measured as 1.84 ± 0.03 nm from optical diffractograms) and were organized into what could be clearly established as discrete crystalline domains (crystallites). From previous WAXS experiments we established that this spacing corresponds to the monomer repeat distance along the chain backbone;[4] hence, the polymer chains run nominally perpendicular to the fringes. The fringes correspond to the regular arrangement of the rigid aromatic and flexible aliphatic segments of the polymer molecules into distinct layers within a crystallite. From these images it was possible to measure the projected size, orientation, and relative population of the crystallites.

To quantify the information in HREM images, boundaries were drawn around individual crystallites on glossy prints by visual inspection. An example of this procedure is shown in Figure 9b. The lateral and axial dimensions were determined by measuring parallel and perpendicular to the (001) fringes, respectively. The results of this analysis are shown in Figure 10 for 46 different crystallites. From these data it was evident that while there was a broad distribution of crystallite sizes, there was a tendency for the crystallites to be somewhat extended in the axial direction. Specifically, the average axial size was 53 ± 23 nm, whereas the average lateral size was 38 ± 13 nm.

From the direction of the lattice fringes within a crystallite it was possible to quantify the orientation distribution with respect to a fixed reference, in this case the edge of the droplet. Figure 11 shows the experimentally measured orientation of the (001) fringes with respect to a line perpendicular to the droplet edge. The data are shown as a function of the distance from the edge of the droplet to the center of the crystallite. The clustering of observations near zero angle indicated a mild preferential orientation of the fringes perpendicular (suggesting the polymer chains are parallel) to the droplet edge. However, at a distances greater than 100 nm from the droplet edge no preferred orientation was found.

Also, it was evident from inspection of the HREM micrographs that near the edge of the droplet there was a large area fraction of the image that contained distinct fringes. To quantify this observation, data were obtained by drawing a series of equally spaced lines on HREM images parallel to the droplet edge and then determining the fraction of each line that passed through a crystallite. Figure 12 shows the fraction of the image that contained lattice fringes as a function of distance away from the droplet edge. Near the droplet edge almost 80% of the image contained fringes, whereas 200 nm into the droplet the population dropped to approximately 25%. Since lattice planes must be oriented parallel to the electron beam to be successfully imaged, the high population of (001) fringes visible to the region near the droplet edge indicated that there was a strong preferential orientation of the polymer chains in the plane of the droplet.

Additionally, there was evidence for structural defects such as pronounced lattice curvature within crystallites as well as grain boundaries between adjacent crystallites. Based on these observations, it is possible to consider the structure of these defects and their potential role in determining material properties. These concepts are addressed in more detail in the following section.

## Discussion

These results provide detailed information about the molecular organization of PMDA-12C during imidization. At the annealing temperature investigated the polymer was 100 °C below the bulk melting point of 312 °C of the polyimide[4] but evidently still had sufficient mobility to organize into discrete crystallites on the order of 50 nm. These domains result in a roughening of the sample surface and a reorganization into regions of higher and lower

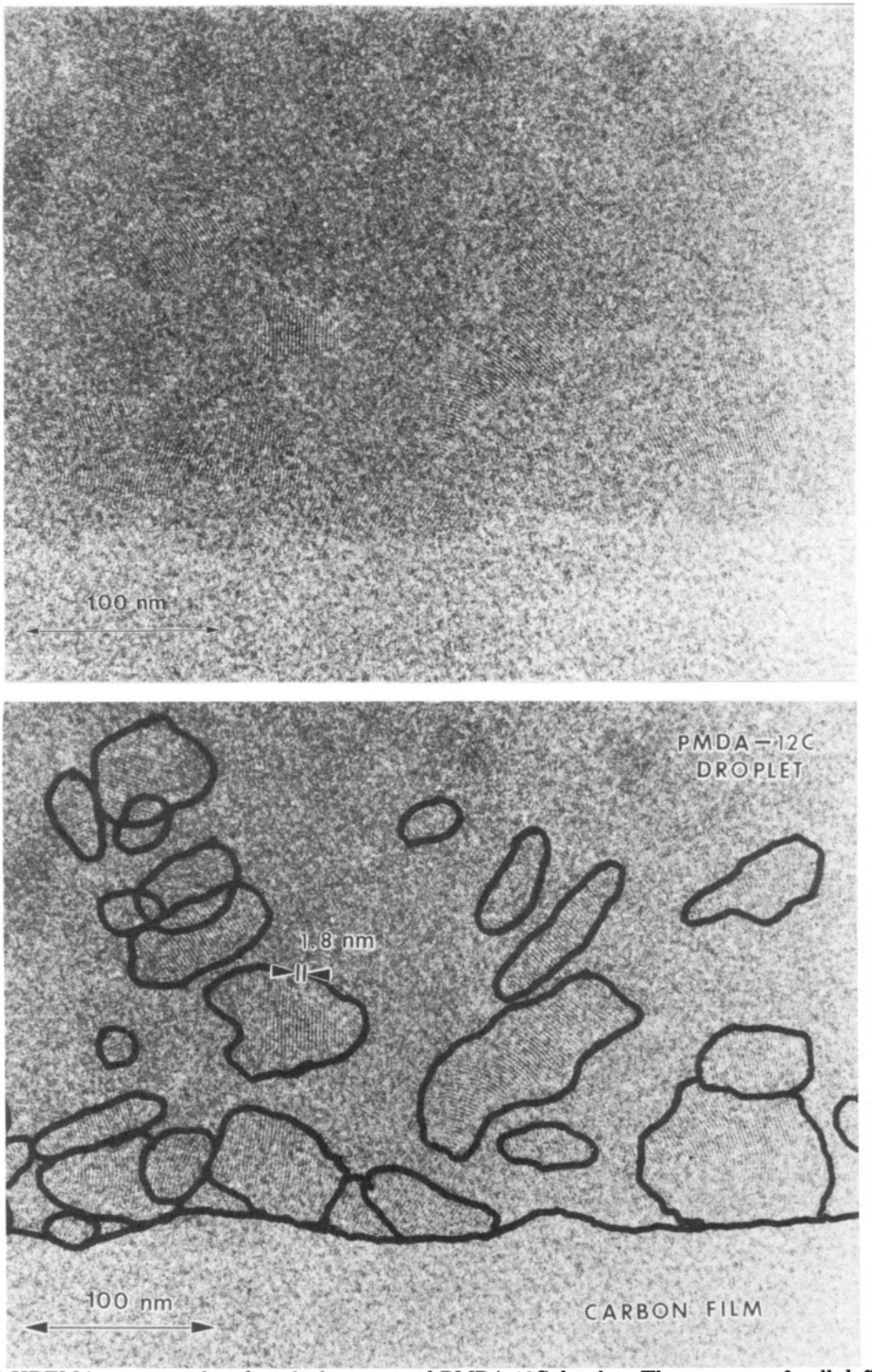


**Figure 9.** (a, Top) HREM image near the edge of a heat-treated PMDA-12C droplet. The presence of well-defined, discrete crystallites can be discerned by regions of uniformly spaced (001) lattice fringes. (b, Bottom) Individual PMDA-12C crystallites as determined by visual inspection. Specific instances of structural defects such as curvature within as well as boundaries between individual crystallites are observed.

density. HREM imaging showed these domains to be crystallites that were slightly more extended in the direction of the polymer molecules. The crystallites imaged by HREM (53 nm axially × 38 nm laterally) were significantly larger than the size determined by WAXS line broadening (7.5 nm). These results emphasize the fact that both crystallite size and internal disorder contribute to the broadening of WAXS peaks. However, experimental evidence for the relative contributions of these effects in crystalline polymers has been lacking because of the difficulty in imaging the crystallites directly.

Our results indicate a preferential orientation of the polymer chains within 100 nm of the droplet edge. There was a weak orientation of the chain axes parallel to the edge of the droplet; quantified by measuring the angle of the (001) lattice fringes as a function of distance from the droplet edge (Figure 11). Also, the observation that a large fraction of the image near the edge contains fringes (80%, see Figure 12) indicates a strong orientation of the polymer chain backbone in the plane of the droplet.

Russell has found evidence for a slight change (~0.05 nm) in the lattice spacings of PMDA-ODA in the outermost

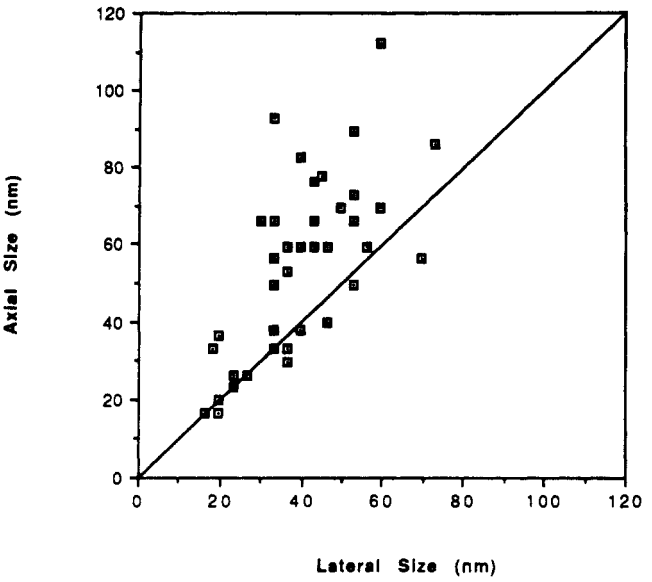


**Figure 10.** Plot of the projected crystallite dimensions measured in the lateral (parallel to fringes) and axial (perpendicular to fringes) directions. There is a distribution of sizes and shapes with a tendency for the crystals to be slightly larger in the axial direction. The average axial size is 53 ± 23 nm, whereas the average lateral size is 38 ± 13 nm.

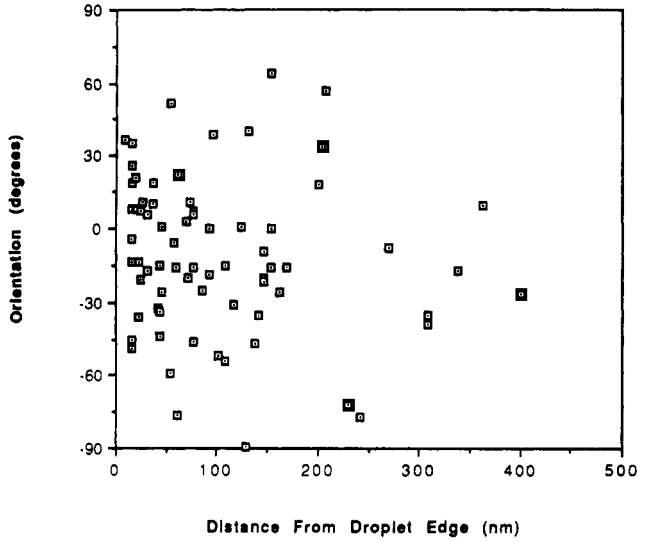


**Figure 11.** Orientation of the (001) fringes with a respect to a line perpendicular to the edge of the droplet as a function of distance away from the edge. There is a mild orientation of the fringes perpendicular to the edge of the outermost 100 nm.

9 nm near a free surface by investigating synchrotron X-ray scattering in the reflection mode as a function of incident angle.[12] Harada et al. were able to detect lattice relaxations near surfaces of silicon crystals from optical transform analyses of high-magnification HREM images.[13] We have looked for similar effects in our micrographs but we were not able to resolve any systematic changes in the lattice spacing as a function of distance away from the droplet edge by optical diffraction. The smallest spot size that could be used for an effective optical diffractogram was 2.5 mm, which corresponds to an area of 100-nm diameter on a 25000× micrograph. Future work involving intermediate negatives or the digitization and numerical Fourier transformation of HREM images near droplet edges may circumvent this problem.

It is worth commenting that we attempted to obtain micro-SAED patterns from the region of the droplet near the edge in order to complement our HREM findings, but

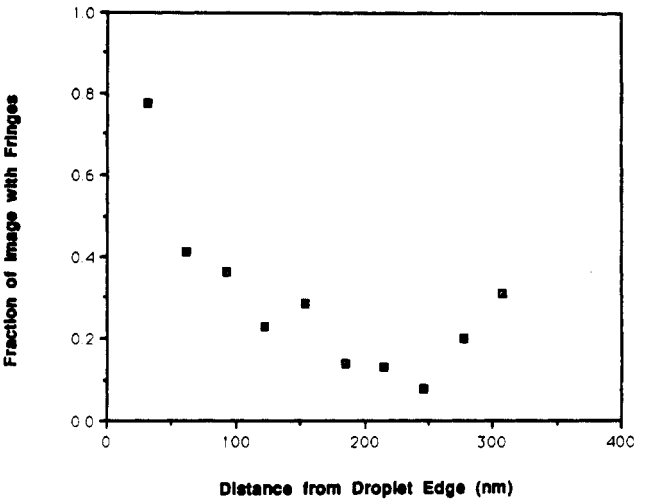


**Figure 12.** Fraction of the image containing fringes as a function of distance away from the droplet edge. Near the edge nearly 80% of the micrograph contains fringes, whereas after 200 nm the lattice lines are seen only 25% of the time.

the electron beam sensitivity of the sample made these experiments problematic. This emphasizes a major advantage of the HREM technique for beam-sensitive samples: once negatives with lattice images have been successfully obtained, it is possible to conduct detailed postimaging analysis to extract useful, highly local information about sample structure.

We have shown that the morphology of poly(imides) cured below their melting point consists of discrete, chain-oriented crystallites, which may contain internal disorder such as bending of the lattice planes. For example, one crystallite in Figure 9 had an internal bending distortion with a radius of curvature of approximately 50 nm, a dimension comparable to the crystallite size. Bending deformations of the (001) planes imply that there is a splay deformation of the chain axes, i.e., a local variation of the backbone orientation. Molecular mechanisms for the accommodation of splay deformations in liquid crystalline polymers in terms of the aggregation of chain ends and folds have been discussed by Mazelet and Klemen.[10]

The TEM micrographs show that the polymer is organized into discrete crystallites that are separated from one another by grain boundaries. Across these boundaries, a large change in local chain orientation may take place. Based on these observations, it is now relevant to discuss the structure of crystallite boundaries in polymers and in particular the important role that chain connectivity should play in these interfacial regions.

In Figures 13 we show a schematic of a crystallite contained within a polymer solid. We first assume that the orientation of the chains within this crystallite is constant and given by a unit vector **c**. We also assume that the density of the crystallite is constant. Now consider a surface $S$ which represents the boundary of this crystallite. From geometrical considerations, there will be a local density of chains per unit area crossing $S$ of the form:

$$\rho_c = \rho_0(\mathbf{n}\cdot\mathbf{c}) \qquad (1)$$

where **n** is a unit vector normal to $S$, $\rho_0$ is the maximum density parallel to **c**, and $\rho_c$ represents the local "flux" of chains at the crystallite surface.

For any arbitrary grain boundary between two different crystallites 1 and 2, each crystallite will have its own characteristic chain flux $\rho_c(1)$ and $\rho_c(2)$, which depend simply on the relative orientations of the crystallites and

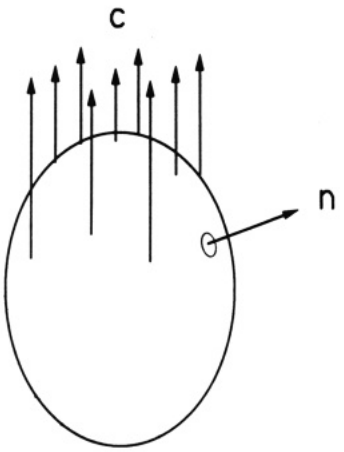


**Figure 13.** Schematic of a chain-oriented crystallite in a polymer solid. The direction of the chains is given by **c**, and **n** is a normal to the crystallite surface. There is a local flux of chains at the surface, which depends upon the angle between **n** and **c**.

the plane of the interface. Now if the chain flux of one crystal at the adjoining boundary is different from that of the other, this requires that the interface has a high population of either ends or bends in the chains associated with the crystal having the higher chain flux.

These purely geometrical considerations have important implications for the expected energetics, structures, and properties of grain boundaries in solid polymers. In the limit of infinite molecular weight, it would be necessary for chains at the interface to bend back into the crystal with the higher chain flux. This constraint would strongly favor interfaces where chain flux remains constant. This simple analysis suggests that the particular types of boundaries observed experimentally should be sensitive to the molecular weight of the sample, the ability of the polymer chain to bend back into the crystallite, and the tendency of the crystallite and grain boundary to maintain a constant density.

For our samples, the relatively low number-average molecular weight of 3560 (number-average degree of polymerization of ~9) suggests that about 20% of the monomers will be at chain ends (2 ends/chain). This rather high density of chain ends should make it more energetically feasible to form grain boundaries where the chain flux is not conserved.

While in our TEM images there seems to be evidence for grain boundaries between crystallites where the chain flux is maintained, there are also instances of boundaries where the chain flux may not be maintained. Figure 14 is an enlargement of a HREM image near the edge of a PMDA-12C droplet and shows support for boundaries where chain flux is maintained (a) and where it is apparently not maintained (b). It may be reasonable to expect that there would be fewer boundaries where chain flux is not maintained as the molecular weight increases. Moreover, grain boundaries where the chain flux is not maintained might be particularly weak, since there would be a large population of chain ends or bends associated with one crystal and therefore inefficient transfer of stress across the interface. Hence, these boundaries may serve as regions where deformation and fracture are initiated. They may also serve as efficient pathways for the transport of small molecules and gases, since both the physical structure and chemistry of the interface may be different than those of the interior of the crystalline domains.

The droplet geometry provides a convenient means to isolate the microstructure of the polymer and minimize complicating effects due to superposition in thick samples.

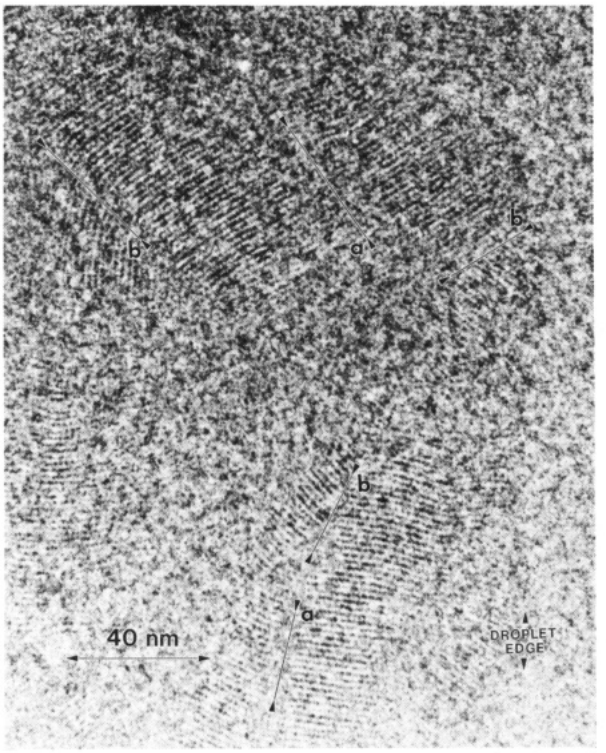


**Figure 14.** Higher magnification view near the droplet edge showing grain boundaries where (a) chain flux is maintained and (b) chain flux is not maintained.

Since the shape and wetting angle of the droplet can be characterized independently by SEM and TEM shadowing experiments, it is possible to obtain estimates of the sample thickness and surface roughness. The position of the droplet edge provides a useful marker for quantifying information about local orientation and other structural parameters. In the future, we anticipate that it should be possible to examine other effects such as substrate composition (which were not investigated in this study) and environment. Particularly interesting would be a substrate with anisotropic surface energetics so that the wetting angle would vary on different edges of the droplet. Of course, the requirement that the substrate be sufficiently thin to enable successful HREM imaging is an important experimental constraint.

## Conclusions

During imidization at temperatures below the bulk melting point, the poly(imide) PMDA-12C organized into discrete crystallites, which caused a roughening of the surface and the development of local density fluctuations. The projected size, shape, relative population, and internal perfection of these crystallites were determined by low-dose HREM of the (001) spacing near the edges of thin droplets. The crystallites were found to be slightly extended in the axial direction, with an average axial dimension of 53 ± 23 nm and an average dimension of 38 ± 13 nm. The high population of (001) fringes near the very edge of the droplet indicated that the polymer molecules were preferentially oriented in the plane of the droplet. There was also a weaker orientation of the chain backbone parallel to the droplet edge. Certain crystallites contained pronounced internal bending deformation, with the apparent radius of curvature of the crystal lattice as small as 50 nm. Evidence for grain boundaries between crystallites was discerned.

**Acknowledgment.** We would like to thank Rudy Angelo for the synthesis of the poly(amic acid) samples used in this study and Connie Osier, Jo Ellen Freida, Kevin Leach, and Brian Cox for their skilled technical assistance.

## References and Notes

(1) Theodorou, D. N. *Macromolecules* **1989**, *22*, 4578.
(2) Henkee, C. S.; Thomas, E. L.; Fetters, L. J. *J. Mater. Sci.* **1988**, *23*, 1685.
(3) Berger, L. L.; Sauer, B. *Bull. Am. Phys. Soc.* **1990**, *35* (3), 509.
(4) Martin, D. C.; Berger, L. L.; Gardner, K. H.; Angelo, R., manuscript in preparation.
(5) Walker, C. C. *J. Polym. Sci.* **1988**, *A26*, 1649.
(6) Kumar, S.; Adams, W. W. *Polymer* **1990**, *31*, 15.
(7) Martin, D. C. Ph.D. Dissertation, University of Massachusetts at Amherst, Amherst, MA, 1990.
(8) Cowley, J. In *High-Resolution Transmission Electron Microscopy and Associated Techniques*; Buseck, P., Cowley, J., Eyring, L., Eds.; Oxford University Press: Oxford, U.K., 1988.
(9) Wrigley, J. *J. Ultrastruct. Res.* **1968**, *24*, 454.
(10) Mazelet, G.; Klemen, M. *Polymer* **1986**, *27*, 714.
(11) Beeston, B. E. P.; Horne, R. W.; Markham, R. Electron Diffraction and Optical Diffraction Techniques. In *Practical Methods in Electron Microscopy*; Glauert, A. M., Ed.; North-Holland: Amsterdam, 1972; Vol. 1, Part 2.
(12) Factor, B. J.; Russell, T.; Toney, M. F. *Phys. Rev. Lett.*, submitted for publication.
(13) Harada, J.; Takata, M.; Miyatake, H.; Koyama, H. *J. Appl. Crystallogr.* **1989**, *22*, 592.